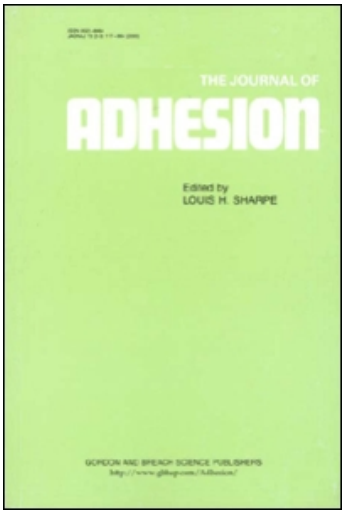

The Journal of Adhesion
Publication details, including instructions for authors and subscription information:
http://www.informaworld.com/smpp/title~content=t713453635

Analysis of Discontinuities in Time-Dependent Adhesive Fracture

H. L. Schreuder-stacer[ab]; R. G. Stacer[a]
[a] Institute of Polymer Science, The University of Akron, Akron, OH, U.S.A. [b] Air Force Astronautics Laboratory, Edwards AFB, California, U.S.A.

To cite this Article Schreuder-stacer, H. L. and Stacer, R. G.(1988) 'Analysis of Discontinuities in Time-Dependent Adhesive Fracture', The Journal of Adhesion, 25: 1, 1 — 21
To link to this Article: DOI: 10.1080/00218468808075438
URL: http://dx.doi.org/10.1080/00218468808075438

J. Adhesion, 1988, Vol. 25, pp. 1–21
Reprints available directly from the publisher
Photocopying permitted by license only

Printed in the United Kingdom

Analysis of Discontinuities in Time-Dependent Adhesive Fracture†

H. L. SCHREUDER-STACER‡ and R. G. STACER

Institute of Polymer Science, The University of Akron, Akron, OH 44325 U.S.A.

(Received May 20, 1986; in final form June 29, 1987)

The adhesive fracture energy of a bond system consisting of a soft adhesive bonded to several elastomers has been evaluated over a wide range of temperature and rate. It was found that the shift factors used to superpose bond data at different temperatures displayed time-dependent features of both the adhesive interlayer and the elastomeric backing/substrate, indicating thermorheologically complex behavior. Individual contributions of the various bond components to the overall response of the joint have been quantitatively described in terms of their weight fractions and plateau moduli. Adhesive fracture energy mastercurves obtained by superposition of data exhibited two pronounced discontinuities. Both of these discontinuities corresponded to changes in adhesive failure mode and one was related to the rubber-to-glass transition of the adhesive. Previous researchers have described the magnitude of this later discontinuity in terms of the simple extension properties of the adhesive. In this work, it is shown that the discontinuity can be described by the thermorheologically complex behavior of the bond system as manifested by changes in the effective viscoelastic reference state.

KEY WORDS Acrylic adhesive joints; EPM or CR or BR backings; adhesive fracture energy; thermorheological complexity; viscoelastic reference state; discontinuity.

INTRODUCTION

The rate and temperature dependence of adhesive failure has been the subject of a number of investigations.[1–11] In most of these

† Presented at the Ninth Meeting of the Adhesion Society, Inc., Hilton Head Island, South Carolina, U.S.A., February 9–12, 1986.

‡ Permanent address: Air Force Astronautics Laboratory, Edwards AFB, California 93523-5000, U.S.A.

studies the method of reduced variables has been successfully employed to develop mastercurves of adhesive strength *versus* temperature reduced crack growth rate. The application of reduced variables to these data suggests a close relationship between the time-dependency of adhesive fracture and small deformation viscoelastic response.[2,12] Unlike the smooth spectrum of common viscoelastic functions, however, adhesive fracture energy curves characteristically exhibit distinct discontinuities.[1–5,8–11] In general, it has been observed that as temperature decreases or rate increases, the discontinuity appears as a drop in fracture resistance, followed by a decrease in the slope of the fracture energy *versus* rate curve. This drop in fracture energy may be as great as 50 percent, and may occur as either an abrupt drop [1–4,9] or span several decades in reduced rate.[5,8,10,11] Associated with these discontinuities is a change in adhesive failure mode, usually described as a transition from cohesive to apparent adhesive failure.

Because of the wide variety of adhesive materials evaluated and differences in test joint configurations employed, it is difficult to develop strong relationships between the discontinuities reported by different researchers. In several cases this change in failure mode has been directly attributed to a characteristic transition of the adhesive layer, *i.e.*, the ductile-to-brittle transition. This later observation has led to attempts to quantify the decrease in fracture strength in terms of simple extension properties of the adhesive,[2,3] As discussed below, this approach fails to account for the relative contributions of other materials to the behavior of a multicomponent bond system.

Improvement of an adhesive system typically depends upon chemical modification of the adhesive layer to increase bond strength. However, it is important to recognize that the measurable bond strength is a property of the entire composite layered system. Consider the process of debonding adhesive tape; the apparent strength of the adhesive depends upon the flexibility and extensibility of the backing material, as well as the deformability of the adhesive layer. These physical characteristics combine with the interfacial bonding capability of the surfaces to determine the strength of the system. Strength measurements of bonded materials are, therefore, influenced by the viscoelastic character of each material which experiences appreciable deformation. Although

many of the above mentioned cases of time-dependent adhesive failure involve only a single deforming substrate, multicomponent bond systems should not be expected to meet the thermorheologically simple requirement necessary for application of the reduced variables method. Thermorheologically simple behavior in this case implies the unlikely situation in which the relaxation times of all the component materials are equally affected by changes in temperature. This paper describes the results of a study to investigate the relative contributions of each deforming layer to the observed strength of the system, with special emphasis on discontinuities occurring in specific regions of temperature and rate.

EXPERIMENTAL

Peel joint preparation and testing

The formulations and cure conditions for the three elastomers used as backing and substrate materials are given in Table I. These include ethylene-propylene rubber (EPM), a crystallization-resistant poly(chloroprene) rubber (CR), and a high-*cis*-poly(butadiene) rubber (BR). The compounded elastomers were pressed into thin sheets, approximately 0·5 mm thick. A smooth bonding surface was

TABLE I
Backing/substrate formulations and cure conditions

Ingredient or conditions	Units	EPM	CR	BR
EPM (Vistalon 404)	phr	100	—	—
CR (Neoprene GRT)	phr	—	100	—
BR (Phillips Cis-4)	phr	—	—	100
Dicumyl Peroxide	phr	2.3	—	1.5
Sulfur	phr	0.32	—	—
Zinc Oxide	phr	—	5.0	—
NA-22[a]	phr	—	0.5	—
Agerite Stalite[b]	phr	—	2.0	—
MgO	phr	—	4.0	—
Cure Temperature	°C	150	150	150
Cure Time	min	120	30	60

[a] Ethylene Thiourea.
[b] Mixture of Octylated Diphenylamines.

produced by curing the sheets against a high gloss photographic plate, and the backing material was rendered inextensible with cloth imbedded into the sheet during cure.

Symmetrical adhesive joints using the three elastomers were prepared as follows. Strips of the elastomers 1 cm wide were bonded to steel shims of the same width using contact cement. These strips shall be referred to as the substrate throughout the remainder of the discussion. A second strip of the same rubber, also 1 cm in width, was used as the backing material. Both substrate and backing were sprayed with a 1:1 mixture of adhesive latex and water. The adhesive used (Flexbond by Air Products, Inc.) was a copolymer of vinyl acetate, 2-ethylhexyl acrylate, and *n*-butyl acrylate in a molar ratio of 60:40 acetate to acrylate. Two lots of this adhesive were employed; these were designated A_1 and A_2. Once dried, the adhesive layer from one spray application was found to be approximately 10 microns thick by weight differences. Sprayed backing and substrate were joined together to produce the symmetrical joint under light pressure, a process found to be independent of pressure. The symmetrical configuration is designated EPM/A_1/EPM, for example, describing the rubber-substrate/adhesive/rubber-backing arrangement.

Asymmetrical joint geometries were also prepared for the EPM and CR elastomer systems to model specific failure modes associated with the previously discussed discontinuity. The first arrangement, designated R/A_1 for rubber-substrate/A_1-backing was made by spraying a thin coat of adhesive on the stiff rubber substrate and adhering a cloth-imbedded strip of adhesive directly onto the sprayed substrate. Arrangement A_1/R was made by affixing an inextensible, sprayed rubber backing onto a cloth-imbedded strip of adhesive bonded to a metal backing plate. In both of these arrangements the adhesive layer was approximately 0.3 mm thick.

Adhesive joints prepared as described were placed in an Instron tensile testing device and the backing material was peeled from the substrate at an angle of 180°. The adhesive fracture energy G_a under these conditions is given through an energy balance approach by

$$G_a = 2\,\mathrm{P/w} \tag{1}$$

where P is the peel force and w is the width of the specimen.

Typically, irregular force fluctuations occurred during peeling. P was determined by averaging the force readings. Each peel joint was subjected to six peel rates ranging from 0.0083 to 4.2 mm/s. Care was taken to initiate adhesive fracture at the substrate/adhesive interface by carefully debonding 1 cm by hand and initiating the test at low rates of peel.

Material characterization

Glass transition temperatures T_g of the various layers of each peel arrangement were determined by slowly cooling 1 mg samples of material to 50°C below T_g and warming the specimens at programmed rates of 5, 10, 15, and 20°C/min in a Perkin Elmer model 1090 DSC/TGA. Values of T_g listed in Table II were obtained by extrapolation to 1°C/min.

Small deformation response properties were measured for each material to determine the temperature dependence of various viscoelastic functions. Although different tests were employed to measure these functions, for thermorheologically simple materials temperature dependence is not influenced by the type of function nor the test method.[12] Stress relaxation modulus $E(t)$ was measured at a variety of temperatures for EPM and CR. Strips of the vulcanized elastomers were strained to 2% at a ramp rate of 83 mm/sec, and the decay in force necessary to maintain this elongation was monitored from 10 to 1000 seconds. Dynamic viscoelastic response was measured with a 30 mm thick disc of adhesive A_1 in the eccentric rotating disc configuration of a Rheometrics Mechanical Spectrometer (RMS) at 2% strain over three decades of rate and a wide range of temperatures. In a slight

TABLE II
Material properties

Materials	T_g (°C)	Density (g/cm^3)	E_e (MPa)	E_N^0 (MPa)
EPM	−65	0.86	1.1	—
BR	−101	1.01	1.0	—
CR	−37	1.24	3.7	—
A_1	−25	1.03	—	0.023
A_2	−33	1.03	—	0.011

variation of dynamic test mode, discs of A_2 and BR were placed in forced dynamic shear between parallel discs in the RMS. Master-curves of viscoelastic response produced from these data are described in a later section.

Tensile equilibrium modulus E_e values for the three elastomers were obtained from the long-time stress relaxation modulus plateau. Corresponding data for the adhesive could not be directly measured since the adhesive was not chemically crosslinked. Instead, for the adhesive the plateau modulus E_N°, associated with physical entanglements,[12] was used. This value was determined by converting dynamic shear modulus plateau data to tensile modulus:

$$E(t) = 3G(t) = 3G'(1/t) \tag{2}$$

where G is the shear modulus, G' is the shear storage modulus, and t is time. These approximate relations are only appropriate in plateau regions where the change in modulus is gradual with time.

RESULTS AND DISCUSSION

Transitions in adhesive failure mode

Adhesive fracture energy was measured as a function of rate and temperature for the three bond systems: EPM/A_1/EPM, CR/A_1/CR, and BR/A_2/BR. All adhesive-to-rubber interfaces were identical in character, as indicated by the preparation methods of the previous section. During peel, the adhesive joints typically fractured by either cohesive rupture within the adhesive layer, failure mode 1 in Figure 1, or clean adhesive failure, modes 2 and 3 in Figure 1. The change from failure mode 1 to 2 is described by Gent and Petrich[3] as a liquid-to-rubber transition, and by Aubrey and Ginosatis[9] as viscous-to-rubber. Transitions from failure modes 2 to 3 have been termed rubber-to-glass by both of these previous research groups.

In the first bond system, failure of the EPM/A/EPM joint characteristically occurred by clean adhesive debonding. Adhesive fracture energy increased with increasing peel rate and decreasing temperature, producing curves of similar shape as shown in Figure 2. At moderate peel rates near room temperature, a knee or peel

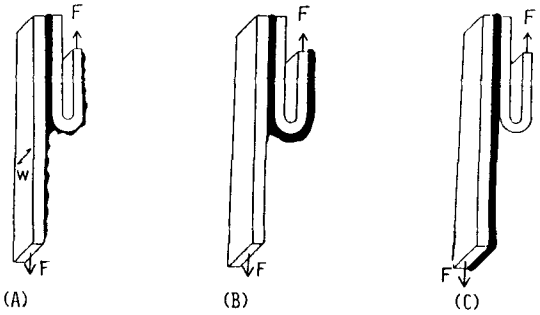

FIGURE 1 180° peel specimens of $R/A/R$ composite: a) failure mode 1; b) failure mode 2; c) failure mode 3.

force plateau was exhibited. At low rates and high temperatures, the adhesive layer preferentially peeled from the rigid rubber substrate and remained attached to the backing. This failure behavior is illustrated as mode 2 in Figure 1. As the peel rate increased and temperature decreased, the failure site changed to mode 3 in Figure 1. At two test temperatures (−10°C and −20°C),

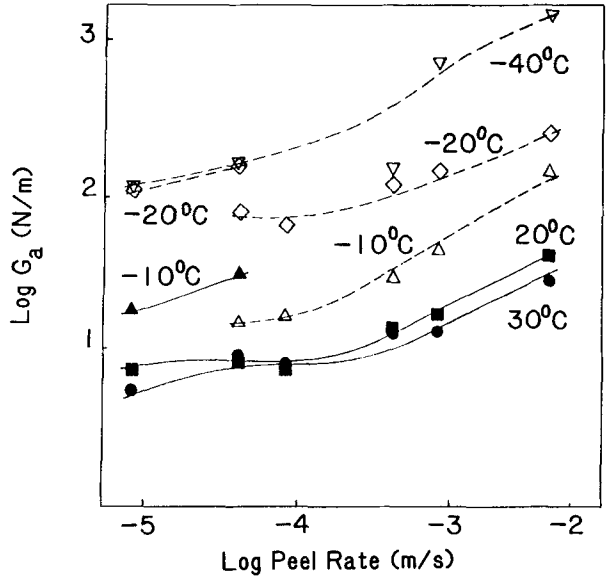

FIGURE 2 Effect of test rate on adhesive fracture energy for EPM/A/EPM. —— and closed symbols, failure mode 2; --- and open symbols, failure mode 3.

the failure site spontaneously switched from failure mode 2 to 3 and remained in mode 3 at subsequently higher rates. In mode 3, the adhesive remained bonded to the flexible substrate, while the backing cleanly stripped away from the adhesive. A significant drop in peel force accompanied this transition. No apparent change in the 180° peel angle accompanied the failure mode shift. Eventually, at lower temperatures failure mode 3 dominated at all rates, despite attempts to initiate failure at the substrate/adhesive interface during setup. Thus, a clear discontinuity was displayed in the general function of increasing adhesive fracture energy with increasing rate.

Behavior similar to EPM was also observed for the CR and BR bond systems. The BR system was found to have nearly the same strength as the EPM system, but the CR bond was an order of magnitude stronger. For both these systems, however, the same change in failure mode occurred between 0 and −20°C, and was accompanied by a drop in G_a. This decrease in G_a was approximately 100 N/m for BR, identical to the EPM bond, while the decrease for the CR system was 1000 N/m, reflecting its order of magnitude greater strength.

Closely associated with the change from failure mode 2 to 3 for these three bond systems is a transition in properties of the adhesive. The change occurs in the temperature region of $T_g + 20$°C for the adhesive, corresponding to the onset of the rubber-to-glass transition. In a previous investigation,[13] the tensile rupture properties of this adhesive were evaluated and a ductile-to-brittle transition in stress-strain response was also observed in this temperature region. Similar adhesive transitions which are associated with discontinuities have been reported by other investigators.[1-3,8,9] It is concluded in this study that the observed failure mode change results from a transition in the response properties of the adhesive. However, it is important to note that the magnitude of the resultant discontinuity cannot be explained in this case by a decrease in the stress capability of the adhesive, since this would imply equal magnitude for all three systems.

Failure mode 1 in Figure 1 was only observed in the CR bond system, and only at the lowest rates and highest temperatures tested. As previously mentioned, the CR bond system was approximately an order of magnitude stronger than the other two bond systems evaluated. This suggests that a critical interfacial

strength between adhesive and rubber must be exceeded before the joint will fail cohesively in the adhesive, as described by Gent and Petrich.[3] During failure mode 1, the adhesive pulled easily apart with residual material adhering to both substrate and backing. Distinct flow lines were visible to the unaided eye on the debonded surfaces after rupture. As rate was increased or temperature was decreased, this liquid-like behavior changed to rubbery behavior and failure mode 2, accompanied by widely fluctuating peel forces, adhesive legging, and irregular crack propagation. A slight drop in adhesive fracture energy was observed as the failure mode changed from cohesive to adhesive. The magnitude of this drop was less than half the size of the discontinuity observed during the mode 2 to mode 3 transition.

No characteristic transition in either adhesive or rubber properties was associated with this second failure mode change. Ellul and Gent[10] have discussed a similar discontinuity in terms of a critical separation rate required for long chain molecules to disentangle. At high rates, they postulate that the speed of diffusion is too slow for disentanglement, resulting in chain breakage. As the separation rate is decreased, however, the chains have sufficient time to disentangle before breaking. Insufficient data exists in our study to verify this mechanism.

As reported above, significant changes in peel joint composition were imposed upon each system studied: the CR joint differed from EPM in both T_g of the rubber layer and strength of the adhesive/rubber bond, while the BR joint differed in only the T_g of the rubber layer, with a slight change in the adhesive T_g. It is now possible to analyze the peel behavior of these composite layered joints and evaluate the effect of two compositional variables, T_g and bond strength, using the reduced variables approach.

Application of reduced variables

The adhesive fracture energy data at different temperatures and rates for the EPM/A_1/EPM bond system in Figure 2 are replotted in Figure 3 as a temperature-reduced mastercurve. A reference temperature, T_s, of 20°C has been arbitrarily selected for this curve. Data obtained from joints that failed in mode 2 are differentiated from those that failed in mode 3 by the solid symbols. No difficulties

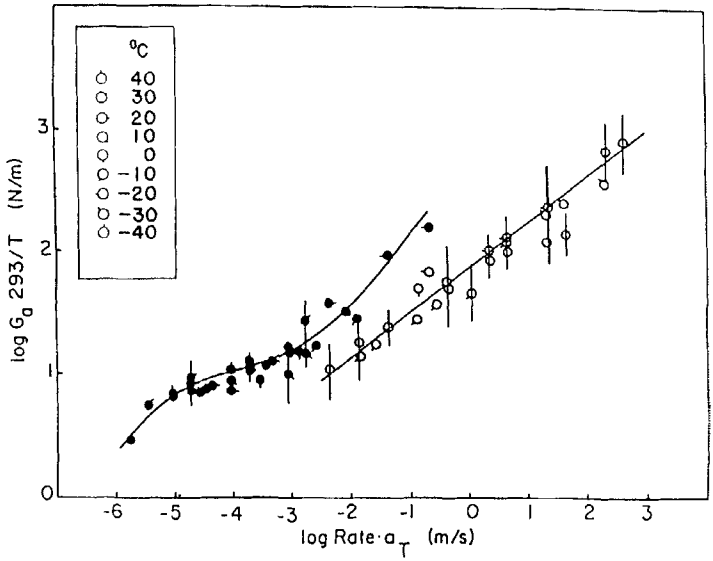

FIGURE 3 Adhesive fracture energy mastercurve of EPM/A_1/EPM. ●, failure mode 2; ○, failure mode 3. $T_s = 20°C$.

nor irregularities were observed in shifting data at different temperatures even though each failure mode produced a distinct curve. The uncertainty of shifting adhesive fracture energy data into a mastercurve was measured by determining a range of acceptable shift distances; shift values employed outside these limits would not produce a smooth curve of adhesive fracture energy.

The apparent discontinuity spans two decades in reduced rate while the aforementioned decrease in G_a of 100 N/m is apparent over this entire span. At high rates beyond this discontinuity, G_a appears as a continuous, monotonically-increasing function. At lower rates, a plateau is evident at 10 N/m, followed by a terminal region in this curve.

Horizontal shift factors, a_T, used to superpose the data at different temperatures into the single curve shown in Figure 3 are given in Figure 4 along with error bars for the empirical shifting procedure. In addition, two lines are shown which represent the shift factors used to superpose small deformation response data for both the adhesive and rubber. As can be seen, the shift factors for

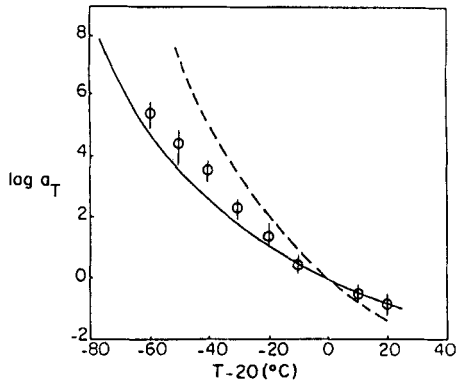

FIGURE 4 Shift factor dependence upon temperature. ○, EPM/A_1/EPM; ——, EPM; ---, A_1.

the composite joint generally fall between these two curves, indicating that the temperature dependency of both the adhesive and rubber contribute to the overall peel joint response.

Quantification of these experimentally derived shift parameters is accomplished through the WLF transform,[14]

$$\log a_T = -C_1(T - T_R)/(C_2 + (T - T_R)) \tag{3}$$

where C_1 and C_2 are experimental constants, T is the test temperature and T_R is a reference temperature. In their original publication,[13] Williams, Landel and Ferry allowed T_R to be an adjustable parameter, usually found to be about $T_g + 50°C$. "Universal" values were used for C_1 and C_2 of 17.5 and 52, respectively. This approach was successful for a number of different polymers. Ferry[12] has since argued that C_1 and C_2 should be experimentally determined for a selected T_R, and then converted to other reference temperatures as desired. In this work, however, the "universal" constants are employed and T_R is used as an adjustable parameter. This approach was selected to visualize better the contribution of the individual materials to the overall behavior of the composite bond joint. Observed deviations from "universal" behavior will be noted in the discussion. It is important to clarify the difference between the reference temperatures used in this report: T_s is any arbitrarily chosen reference temperature used for data presentation; T_R is a reference state, related to the T_g of a system.

Returning to the data in Figure 4, the $T_R - 50°C$ values used to describe the data were −69, −60 and −35°C for the EPM, composite bond, and adhesive, respectively. The EPM and A_1 values are within reasonable agreement with the glass transition temperatures given in Table II. Both the EPM and adhesive shift factors from small deformation response testing were fully described using the "universal" constants and these fitted T_R values.

In addition to the symmetrical EPM and CR bond systems, asymmetrical joints A_1/R and R/A_1 were also tested at a variety of temperatures and rates. Recalling a previous investigation,[13] mastercurves from these asymmetric joints agreed well in terms of slope and absolute magnitude of fracture energy with the regions in Figure 3 they were intended to model. This included the failure mode 1 to 2 transition in the CR bond system, which also occurred in the asymmetrical joints. The only discrepancy occurred with the joint R/A_1, intended to model failure mode 2. In this case, the measured fracture energy was significantly higher than in the symmetrical joint, a fact which was attributed to the thicker adhesive layer required to construct the sample. The fitted reference temperatures for the behavior of these two asymmetric joints are presented in Table III for comparison. These values also tend to fall between the response of pure adhesive and pure rubber, with the substrate contributing less in all cases.

TABLE III
Reference temperature for composite peel joints and component materials

Material/composite joint	DSC T_g(°C)	Experimental $T_R - 50$(°C)	Derived $T_R - 50$(°C)
EPM	−65	−69	—
A_1/EPM	—	−64	—
EPM/A_1/EPM	—	−60	−57
EPM/A_1	—	−39	—
A_1	−25	−35	—
CR	−37	−45	—
A_1/CR	—	−45	—
CR/A_1/CR	—	−35	−39
CR/A_1	—	−35	—
BR	−101	−135	—
BR/A_1/BR	—	−90	−90
A_2	−33	−42	—

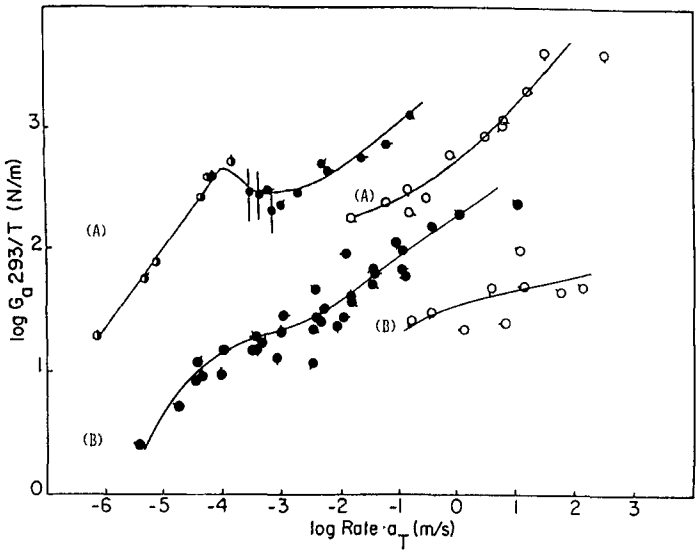

FIGURE 5 Adhesive fracture energy mastercurve of a) CR/A_1/CR and b) BR/A_2/BR. ◑, failure mode 1; ○, failure mode 2; ●, failure mode 3. $T_s = 20°C$.

Figure 5 presents the adhesive fracture energy mastercurves referenced to 20°C for the BR and CR symmetrical bond systems. Treatment of these data was identical to that previously described for the EPM system. The mastercurve for BR/A_2/BR is very similar to the EPM curve in Figure 3 in terms of shape and magnitude. As with EPM, the discontinuity spans two decades in reduced rate, the decrease in G_a is approximately 100 N/m, and a plateau is apparent in the low-rate region. Data in the high-rate region are not as complete because the high-*cis* BR elastomer crystallized at temperatures below −40°C, resulting in a different peel angle.

The CR/A_1/CR bond mastercurve shows an order of magnitude greater fracture resistance, as previously mentioned. Shape features of this curve are very similar to those of the curves of the other bond systems except in the low-rate region. This is the reduced rate region where the transition from failure mode 1 to 2 occurred. Data obtained from peel joints displaying mode 1 failures are designated by half-open symbols. This discontinuity appears similar to the higher rate one; however, it is more abrupt and of significantly

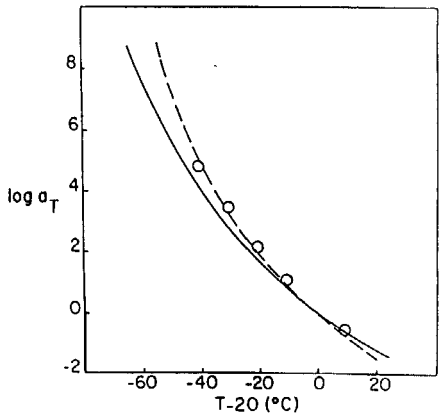

FIGURE 6 Shift factor dependence upon temperature. O, CR/A_1/CR; ——, CR; ---, A_1.

lower magnitude than discontinuities occurring between modes 2 and 3.

Figures 6 and 7 present the shift factors used to superpose bond fracture energy data in Figure 5, along with those used to superpose small deformation response properties of the corresponding bond components. Data are presented as before for EPM and T_R values are tabulated for comparison in Table III. As was the case with

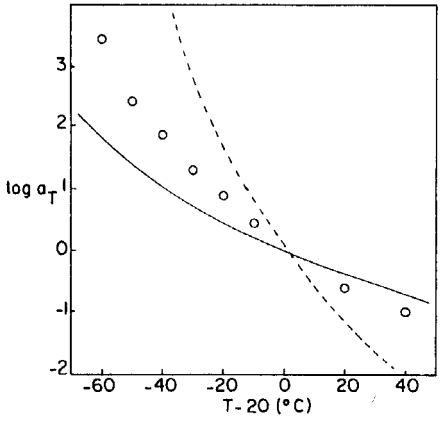

FIGURE 7 Shift factor dependence upon temperature. O, BR/A_2/BR; ——, BR; ---, A_2.

EPM, the response of the BR bond system falls in between the response of its individual bond components. The shift factors for the CR/A_1/CR composite bond system come very close to the response of the pure adhesive. This implies that the CR elastomer contributes less to the temperature dependency of the bond system than either EPM or BR.

Application of the WLF equation with universal constants for a series of materials implies that the change in free volume with temperature is the same for each material; only the reference temperature or state changes. This assumption is tested in Figure 8. Here the data in Figures 4, 6 and 7 are normalized for their effective reference temperature. Experimentally derived shift factors for the composite joints are shown as individual symbols, while the WLF equation is illustrated by the solid line. Agreement is good except for a slight deviation in high temperature EPM joint data, indicating that this assumption is a reasonable one.

In evaluating the data in Table III, it is surprising to note that the adhesive layer contributes more to the effective reference state of the composite joint than would be predicted from a simple rule of additive free volume. Approximately 100 times more rubber than adhesive is used in these joints. In addition, and perhaps more

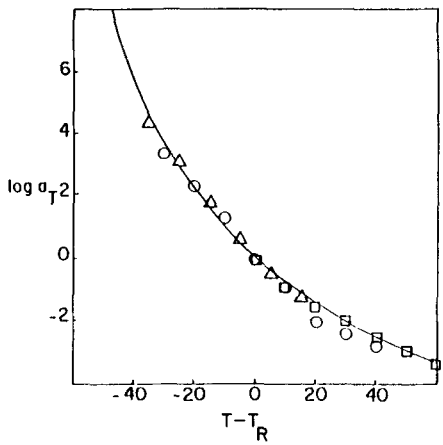

FIGURE 8 Shift factors for all composite joints and component materials plotted with respect to individual reference temperatures. —, WLF equation; ○, EPM/A_1/EPM; △, CR/A_1/CR; □, BR/A_2/BR.

important to the applicability of reduced variables, is the fact that the viscoelastic behavior of both the adhesive and the rubber combine to produce a thermorheologically complex joint. An attempt will be made to explain and quantify these observations below.

Effective joint reference state

It is now possible to discuss the master curves of adhesive fracture energy (Figures 3 and 5) in terms of their effective reference state. At temperature and rate conditions corresponding to failure mode 2, the adhesive and rubber are clearly contributing to the response. Since the modulus of the adhesive is approximately two orders of magnitude lower than the rubber, most of the deformation occurs in the adhesive. In failure mode 3, however, the adhesive has transitioned to a glass and deformation is minimal, while the rubber response continues as before. This clearly indicates a need to correct the mastercurve for a change in effective viscoelastic reference state. To accomplish this, the T_R of the rubber can be used for adhesive fracture energies obtained from joints failing by mode 3. Support for this approach comes from limited data for the EPM/A_1/EPM composite joint tested below the T_g of the adhesive. Low temperature data in Figure 4 suggest that the joint response nears that of the rubber. As illustrated in Figures 9–11, assigning different reference temperatures to the different failure modes superposes the two curves previously plotted in Figures 3 and 5 and eliminates the discontinuity. This indicates that the discontinuity is not the result of a decrease in adhesive strength but, rather, the result of a change in effective reference state.

A change in reference temperature of only a few degrees could also eliminate the low-rate or high-temperature discontinuity in the CR bond master curve. As previously discussed, however, no characteristic material transition nor verifiable mechanism can be related to this discontinuity. Consequently, no attempt was made in this study to explain this discontinuity quantitatively.

A number of attempts have been made to quantify the relative contributions of two or more homopolymers to the effective reference state of a copolymer or blend.[14–19] All of these approaches rely on some form of weighted average or volume rule of

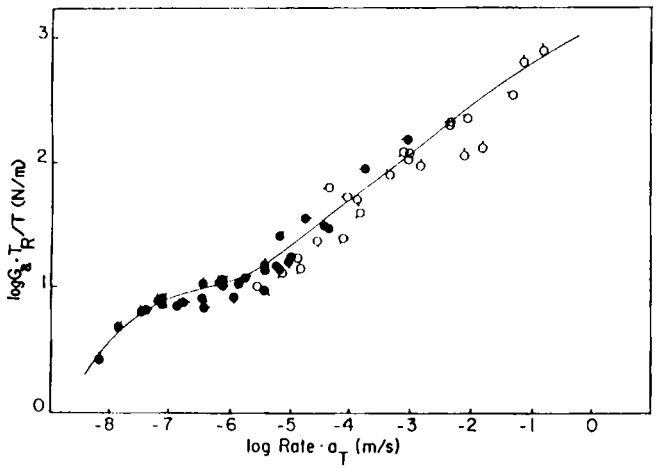

FIGURE 9 Adhesive fracture energy mastercurve of EPM/A_1/EPM plotted to reference temperatures of each failure mode. ●, failure mode 2 with $T_R = -60°C$; ○, failure mode 3 with $T_R = -69°C$.

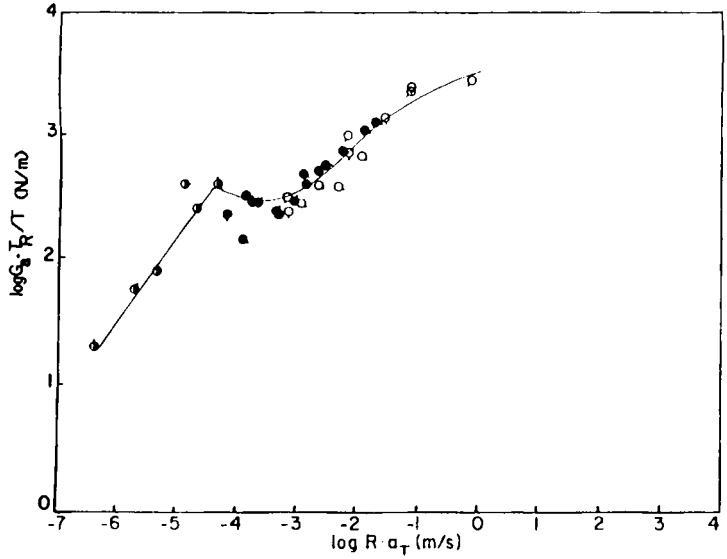

FIGURE 10 Adhesive fracture energy mastercurve of CR/A_1/CR plotted to reference temperatures of each failure mode. ◑; failure mode 1 with $T_R = -35°C$; ●, failure mode 2 with $T_R = -35°C$; ○, failure mode 3 with $T_R = -45°C$.

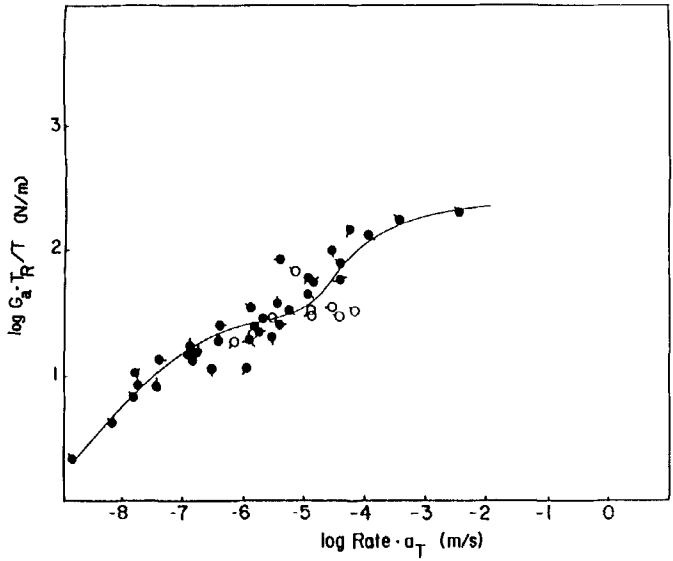

FIGURE 11 Adhesive fracture energy mastercurve of BR/A_2/BR plotted to reference temperatures of each failure mode. ●, failure mode 2 with $T_R = -90°C$; ○, failure mode 3 with $T_R = -135°C$.

additivity. With the exception of those equations that use empirical fitting parameters, none of these models describe the T_R data for the composite joints in Table III. In addition to these efforts to predict intermediate glass transition temperatures for copolymers, Takayanagi[20] and others[21–23] have developed mechanical models for multi-phase polymeric systems which attempt to explain the thermorheologically complex behavior exhibited by these materials. Using the simplest of these mechanical models, two materials deformed in series, it can be show that at equal weight fractions the lower modulus material dominates the combined response, proportional to their relative moduli. This explains the greater contribution of the adhesive to the composite T_R than would be predicted by a volume rule of additivity since, as shown in Table II, the adhesive is significantly softer than the rubbers in their respective plateau regions. The mechanics of peel adhesion are generally analyzed using elementary beam bending theory. A number of basic assumptions are made which lead to relationships such as Eq. (1).[25] Among these are the concept that the applied peel force is parallel to the

bond plane while the actual bond separation force acts in tension perpendicular to this plane. As a consequence, in the localized region around the advancing separation front, joint response can be viewed as three viscoelastic materials (backing, adhesive and substrate) deformed in series, and is used in this manner to apply the rule of mixtures to this region.

Simple linear addition of fractional free volumes predicts the intermediate T_g of a two component system to be:[21]

$$T_g = T_{g1} + w_2(T_{g2} - T_{g1}) \tag{4}$$

where T_{g1} and t_{g2} are the glass transition temperatures of the two components, and w_2 is the weight fraction of the second component. In order to account for differences in response due to excitation of the two components, Eq. (4) can be rewritten as:

$$T_R = T_{R1} + w_2^*(T_{R2} - T_{R1}) \tag{5}$$

where T_{R1} and T_{R2} are the reference temperatures of the two components, and w_2^* is the modulus-normalized weight fraction given by:

$$w_2^* = (w_2/E_2)/((w_2/E_2) + (w_1/E_1)) \tag{6}$$

where w_1 and w_2 and E_1 and E_2 are the weight fractions and moduli of the two components, respectively.

Application of Eq. (5) to the symmetrical joints is shown by the derived T_R values in Table III. Agreement is excellent in all three cases, with none of the predicted values varying from experimental by more than four degrees. In order to make these predictions, it was necessary to assume that the equilibrium and plateau moduli in Table II completely describe the respective rheological behavior of the individual materials. Incorporation of both the substrate and backing into Eq. (6) was accomplished by doubling the corresponding weight fraction, since both substrate and backing were of equal thickness and of the same material in all the symmetrical bonds.

Application of Eq. (5) to the asymmetrical joints is less successful. The equation predicts the same T_R value for both R/A and A/R bonds. Table III clearly shows that this is not the case. Data for both the EPM and CR systems indicate that the substrate contributes little to temperature response of the composite joint. In fact, for the CR asymmetrical joints, no significant contribution of the

substrate was observed. This is probably due to the close proximity of the reference temperatures of the two materials. Additional work will be required before Eq. (5) or one like it can be used to predict T_R values for asymmetrical joints without resorting to empirical fitting parameters.

CONCLUSIONS

1. Two discontinuities in time-dependent adhesive fracture energy curves have been observed for a bond system consisting of a soft adhesive bonded between several elastomers. Associated with both of these discontinuities is a distinct change in adhesive failure mode. Both discontinuities are characterized by a dramatic decrease in adhesive fracture energy, followed by a decrease in the slope of the fracture energy *versus* reduced rate curve. These failure mode changes are consistent with those described by previous researchers[3,9] using different materials.

2. The low-temperature or high-rate discontinuity, which was observed in all three elastomeric systems tested, has been related to the rubber-to-glass transition of the adhesive interlayer. No characteristic transition in properties of either the adhesive or rubbers was associated with the high-temperature or low-rate discontinuity. This later discontinuity was only observed in one of the composite bond systems tested.

3. It has been found that the shift factors used to superpose bond data at different temperatures displayed time-dependent features of both the adhesive interlayer and the elastomeric backing/substrate, indicating thermorheologically complex behavior. The temperature dependency of the composite joint falls somewhere in between the response of the pure rubber and adhesive. Relative contributions of the various bond components to the overall response of the joint have been quantitatively described in terms of their weight fractions and plateau moduli.

4. It has been shown that the largest of the two discontinuities in time-dependent adhesive fracture can be explained in terms of this thermorheologically complex behavior of the bond system. Specifically, it is surmised that the effective reference temperature of the composite adhesive joint changes during failure mode transitions.

These reference temperatures quantify the temperature dependency of the dominant viscoelastic mechanism controlling each system. Assignment of different reference temperatures to different regions of the mastercurves superposes the data and eliminates the discontinuity.

Acknowledgement

This work was performed at the facilities of the University of Akron's Polymer Science Institute under the guidence of Prof. A. N. Gent, whose helpful suggestions are gratefully appreciated. One of us (HLS) would like to acknowledge receipt of a fellowship by the Adhesive and Sealant Council as well as support by Johnson and Johnson Products, inc.

References

1. W. M. Bright, in *Adhesion and Adhesives,* J. Clark, J. E. Rutzler and R. L. Savage, Eds. (Wiley, New York, 1954).
2. D. H. Kaelble, *J. Coll. Sci.* **19,** 413 (1964).
3. A. N. Gent and R. P. Petrich, *Proc. R. Soc. London* **A310,** 433 (1969).
5. B. W. Cherry and K. W. Thomson, in *Aspects of Adhesion,* Vol. **6,** D. J. Alner, Ed. (University of London Press, London, 1971).
6. A. N. Gent and A. J. Kinloch, *J. Polym. Sci. Phys. Ed.* **9,** 659 (1971).
7. E. H. Andrews and A. J. Kinloch, *Proc. R. Soc.* **A332,** 385 (1973).
8. D. W. Aubrey and M. Sherriff, *J. Polym. Sci.* **18,** 2597 (1980).
9. D. W. Aubrey and S. Ginosatis, *J. Adhesion* **12,** 189 (1981).
10. M. D. Ellul and A. N. Gent, *J. Polym. Sci. Phys. Ed.* **22,** 1953 (1984).
11. M. D. Ellul and A. N. Gent, *ibid.* **23,** 1823 (1985).
12. J. D. Ferry, *Viscoelastic Properties of Polymers, 3rd Edition,* (Wiley, New York, 1980).
13. H. L. Stacer, Ph.D. Dissertation, The University of Akron, 1987.
14. M. L. Williams, R. F. Landel, and J. D. Ferry, *J. Am. Chem. Soc.* **77,** 3701 (1955).
15. M. Gordon and J. S. Taylor, *J. Appl. Chem.* **2,** 495 (1952).
16. F. Jenckel and R. Heusch, *Kolloid. Z.* **30,** 89 (1953).
17. T. G. Fox, *Bull. Am. Phys. Soc.* **1,** 123 (1956).
18. L. A. Wood, *J. Polym. Sci.* **28,** 319 (1958).
19. P. R. Couchman, *Macromolecules* **11,** 1156 (1978).
20. T. K. Kwei, *J. Polym. Sci., Polym. Lett. Ed.* **22,** 307 (1984).
21. M. Takayanagi, *Proceedings of the 4th International Congress of Rheology, Part 1,* E. H. Lee and A. L. Copley, Eds. (Wiley, New York, 1965).
22. D. H. Kaelble, *Trans. Soc. Rheol.* **15,** 235 (1971).
23. D. G. Fesko and N. W. Tschoegl, *J. Polym. Sci. C,* **35,** 51 (1971).
24. D. G. Fesko and N. W. Tschoegl, *Int. J. Polym. Mater.* **3,** 51 (1974).
25. D. H. Kaelble, *Trans. Soc. Rheol.* **4,** 45 (1960).